Proceedings of the Indian National Science Academy (2024) 90:442–455
https://doi.org/10.1007/s43538-024-00280-3

REVIEW ARTICLE

Internal structure of India: perspectives from a review of the seismological imaging studies from 2020 to 2023

Himangshu Paul[1] · **Vineet K. Gahalaut**[1]

Received: 29 December 2023 / Accepted: 11 March 2024 / Published online: 8 April 2024

Abstract
The Indian subcontinent is a mosaic of different provinces exhibiting diversity in age, geology, elastic strength, tectonics, and seismicity. The evolution of most of the provinces from the Archean to the present age is not yet fully understood, which is further complicated by the active continent–continent collision along the northern margin and other intraplate forces. Seismological imaging helps unravel various subsurface structural features, thereby enabling a better understanding of the tectonic evolution. In the last 4 years, several seismological imaging studies have been carried out by Indian scientists, which has resulted in a remarkable improvement in depth estimation and constraining the geometry of important discontinuities, such as the Main Himalayan Thrust (MHT) and the Moho. Since the MHT plays an important role in generating megathrust earthquakes in the Himalaya, a large number of studies have been carried out in the Himalaya and their number almost equals the combined studies carried out in the rest of India. Detailed velocity structure of the crust and mantle has been estimated by tomographic inversion throughout the Indian subcontinent, even including Tibet, Pamir and Burma in certain cases. Attempts have also been made to estimate the depth and topography of deeper structures such as Hales discontinuity, Lithosphere–Asthenosphere Boundary, Mantle transition zones, and D'' layer over the Core Mantle Boundary. Some of the studies have developed and adopted newer methodologies to map the structure. Those studies are analysed here to provide an overview of the progress toward understanding the structure.

Keywords Receiver function · Tomography · Indian Shield · Himalaya · Crust-Mantle structure · Main Himalayan Thrust

Introduction

The earth has been tectonically evolving for billions of years and one of the most efficient ways of understanding this evolution is through geophysical investigation. In India, diverse tectonic evolutionary modes are present, which include continent-continent collision in the northern margin, reactivated rift zone in the Kachchh and subduction features in the Indo-Burma and Andaman arcs. Moreover, there are regions within the Indian subcontinent which host evolutionary evidence from the past, such as the presence of Archean crust in the Singhbhum craton of the Eastern Indian Shield region and Cretaceous volcanism in the South Indian Shield. The imprints of tectonic evolution must be embedded within the structure, so a knowledge of the detailed structure is essential for a deeper understanding.

Seismological signals, which include travel times of different phases and amplitudes, are analyzed to visualize deeper structures of the earth with sufficient resolution and reliability. In recent years, various seismological tools have been developed to improve the accuracy and resolution further. Seismological imaging is a common term to signify the application of various seismological tools to understand the internal structure of the earth. Seismological imaging can provide information about the elastic velocity (related to composition), approximate dimension and geometry of subsurface layers. In the last 4 years (2020–2023), several seismological imaging studies have been carried out in India from regional to local scale, contributing to a better understanding of the subsurface structure of the Indian subcontinent. A common seismological imaging tool to identify and estimate the depth of different discontinuities (chemical, petrological and mechanical) is receiver function analysis, where the converted phase properties are utilised to map the

✉ Himangshu Paul
heman2007s@gmail.com

[1] CSIR-National Geophysical Research Institute, Hyderabad, India

discontinuity beneath the receiver. Another popular methodology is the tomographic inversion, where the velocity of the medium is iteratively adjusted to minimise travel time errors of different phases. Receiver function analysis and tomography seem to be the most popular choice for Indian scientists for seismological imaging. A brief note on the various seismological imaging tools is given in Appendix A.

In this study, we have tried to compile and analyze most of the recent seismological imaging studies to present an overview of the progress made. We have included contributions from Indian scientists only. We have restricted ourselves to seismological imaging only and allied seismological fields like anisotropy, source characteristics, hazard, etc., are excluded. Within our restrictions, we have tried to be as exhaustive as possible, and any omission is unintentional. In the last 4 years, seismological imaging studies in India have focused on mapping the decollement between the underthrusting Indian Plate and the Himalayan wedge, also known as the Main Himalayan Thrust (MHT). It is important because the decollement hosts the most destructive (great and major) earthquakes and understanding its geometry may assist in improved hazard assessment and mitigation. Estimating the variation of Moho depth is another important objective seen in most studies. In stable parts of India, attempts have been made to observe the detailed velocity variation in order to identify anomalous or significant structures. A few studies have attempted to map the deeper structures, such as the lithosphere boundary or mantle transition zones. We analyse and present the seismological imaging studies region wise. Frequently used abbreviations in the text are listed in Appendix B.

Himalaya

Uttarakhand Himalaya

Uttarakhand Himalaya is situated in the central seismic gap between the meizoseismal zones of the 1505 Nepal earthquake and the 1905 Kangra earthquake (Bilham and Wallace 2005). A seismic gap represents a region where accumulated slip due to convergence greatly exceeds the slip due to past great and major earthquakes in the region, resulting in a greater potential and probability of large earthquakes. It piqued the interest of several organizations and large seismological networks were independently established in the region. These data were useful in imaging the crust and lithosphere beneath the Uttarakhand Himalaya.

Receiver Function (RF) inversion and Common Conversion Point (CCP) stack along an approximate N-S profile in the eastern margin of Uttarakhand showed that the depth of the Moho varies from 38 to 42 km (Hazarika et al. 2021). Additionally, this study revealed the Main Himalayan Thrust (MHT) ramp structure and a low velocity zone (LVZ) in the lower crust beneath the Higher Himalaya. Along a profile in a similar location but with dense stations, Madhusudhan et al. (2022) calculated P_n and S_n velocities to show that they are different in updip and downdip direction implying that the Moho dips northwards by ~3.5°. Along a NE-SW profile, about 150 km west of the previous profile, Kanna and Gupta (2020) performed RF modelling of 16 stations to show that the Moho deepens steeply (~5°) northward and its depth varies between ~45 km and ~58 km. This study agreed on the flat-ramp-flat structure of the MHT but reported high velocity of the lower crust in the Higher Himalaya.

The above studies reported depth variation along linear profiles. However, Mandal et al. (2021a) performed RF H-κ (H = crustal thickness, $\kappa = V_P/V_S$) stack of 42 stations which were distributed in a 150 km × 300 km area across Kumaon–Garhwal Himalaya. This study reported H varying from 28 to 54 km and extreme variation of Poisson's ratio (σ) between 0.17 and 0.36. σ is related to κ (see Appendix A). This study also reported alternating thinning and thickening of the crust from west to east in Uttarakhand. For a similar set of stations, RF CCP stack (Mandal 2023) and joint inversion of RF with surface wave (SW) dispersion (Mandal et al. 2023) showed that the MHT lies at 12-21 km depth, the Moho dip northeastward with its depth varying between 30 and 55 km and the Lithosphere–Asthenosphere Boundary (LAB) depth varies from ~130 to 180 km. This study proposed that the Uttarakhand Himalaya is segmented by several ~N–S trending transverse structures. Another joint inversion study (Ashish et al. 2023), using different sets of stations in Kumaon-Garhwal Himalaya found similar estimates—MHT flat-ramp-flat structure with its depth varying from 8 to 24 km, the Moho depth varying from ~50 to 60 km and marked thinning of the crust in the eastern part of the Garhwal Himalaya.

RF studies provide a reliable estimate of the depth of the discontinuities but velocity estimations are less constrained. An accurate and reliable velocity structure can be obtained by tomography. Local earthquake tomography studies in the Uttarakhand Himalaya (Gupta et al. 2022; Mandal et al. 2022), using different sets of stations and different sets of earthquakes, made similar observations. Both the studies observed (i) the presence of low-velocity sediments above the basement, (ii) a heterogeneous velocity structure in the upper crust, and (iii) a low velocity layer representing the MHT (Fig. 1). Both the studies associated regions of low V_P and high V_P/V_S ratio within the MHT with the presence of fluids and locales for earthquake generation. Ambient Noise Tomography (ANT) of a larger region, including the Uttarakhand Himalaya and Himachal Himalaya (Verma et al. 2023), made similar observations, such as low-velocity sediments, low-velocity MHT, presence of fluids and its association with seismicity. Additionally, this study identified a

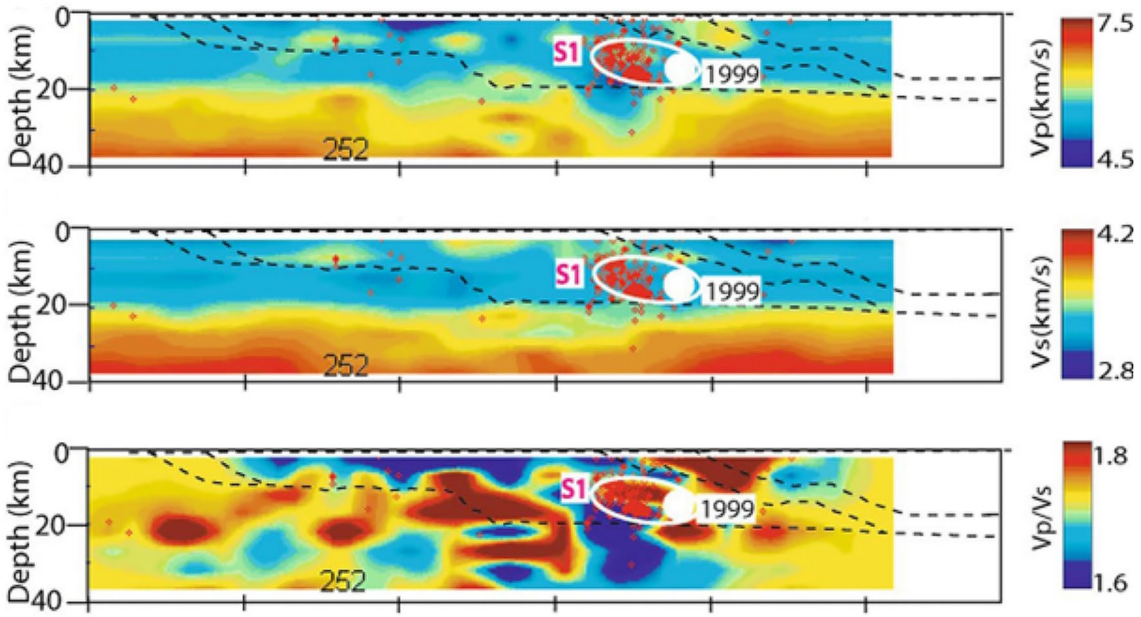

Fig. 1 The V_P, V_S and V_P/V_S variation in the Uttarakhand region is shown in a cross-section along an NE-SW profile (reproduced from Mandal et al. 2022). The major thrust boundaries are schematically marked by dashed lines. The 252 local earthquakes are represented by red circles, while the white-filled circle represent the 1999 M_W 6.4 Chamoli earthquake. The elliptical area (S1) demarcates regions of low V_P, low V_S and high V_P/V_S, possibly indicating the presence of fluids

high-velocity structure close to the MHT, possibly associated with a duplex structure.

Seismic attenuation studies (Monika et al. 2020; Sivaram and Gupta 2022) carried out in Kumaon–Garhwal Himalaya observed different attenuation in the Lesser and Higher Himalaya. Monika et al. (2020) reported higher attenuation in the Kumaon region compared to Garhwal. It is seen that the velocity and attenuation structure is very heterogeneous within the Uttarakhand Himalaya, especially going from the west to the east. The velocity values of important structures such as MHT and Moho and their actual depths vary from one study to another. In this respect, sometimes a 1D model becomes more suitable than a varying 3D velocity structure. Kanaujia et al. (2023) built an optimal 1D velocity structure for the Uttarakhand Himalaya using Monte Carlo-style inversion which is able to reduce residuals during earthquake locations.

Northwestern Himalaya

The northwestern Himalaya consists of Himachal, Jammu & Kashmir (J & K), and Ladakh regions and is important in the sense that a seismic gap is postulated between the meizoseismal zones of the 1905 Kangra and the 2005 Kashmir earthquakes. RF modelling of 15 stations along a profile close to the Himachal Himalaya revealed that the depth of the Indian Moho increases from ~46 km in the Indo-Gangetic Plains (IGP) to ~78 km in the Karakoram (Kanna and Gupta 2021). This study associated a low-velocity intracrustal layer as the MHT and identified a high velocity lower crust in the Higher Himalaya possibly due to partial eclogitization. Similarly, based on RF CCP stack and joint inversion of RF with SW dispersion, Mitra et al. (2023) observed the deepening of the Moho from ~45 km to ~70 km northwards in J & K Himalaya. This study reported the MHT LVL to have a flat-ramp-flat geometry and identified a duplex structure in the Lesser Himalaya. It also reported the existence of strong lateral variation from the west to the east in the J & K Himalaya.

Kumar et al. (2022) provided a high-resolution 3D V_S model of the crust by SW and AN tomography across a large region encompassing the northwestern Himalaya, western Tibet and Pamir–Hindu Kush ranges. This study showed that the Moho depth varies from 50 to 80 km northwards and that the northern limit of the Indian crust lies near the Qiangtang Block in western Tibet and beneath central Pamir, further west (Fig. 2). This study reported the continuation of mid-crustal LVZs across the Himalaya and Karakoram fault and its discontinuous patches in western Tibet and Pamir, associated with different sources. A seismic attenuation study in NW Himalaya (Mishra et al. 2020) reported that the frequency-dependent attenuation of the P-, S- and Coda waves are highest in the lesser Himalaya, followed in order by those in the sub-Himalaya, Indo-Gangetic Plains and Higher Himalaya. A similar study (Kumari et al. 2020) in the Kinnaur region of Himachal Himalaya shows higher attenuation in the Tethys Himalaya compared to the Higher

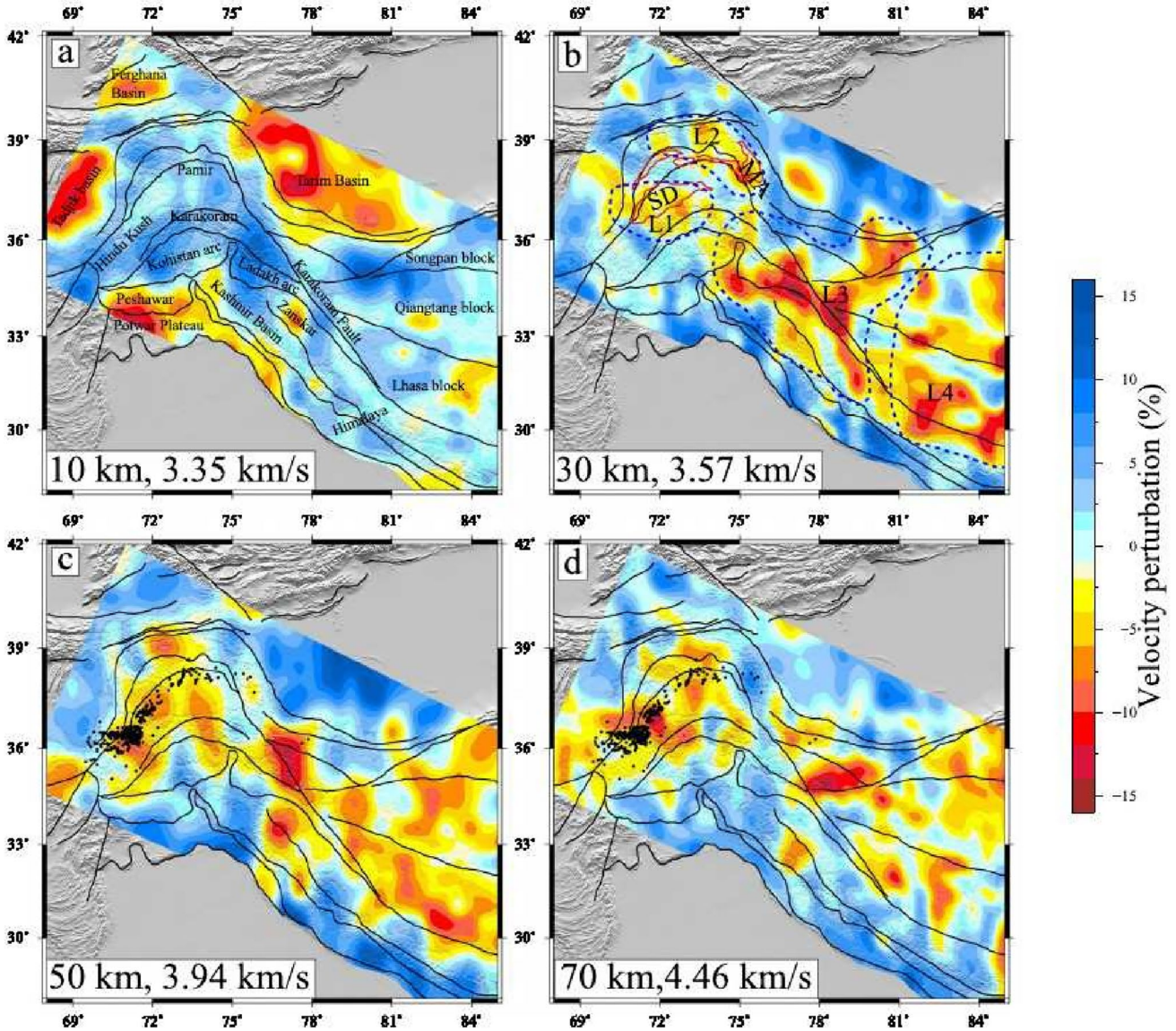

Fig. 2: 3D V_S variation in the NW Himalaya, Tibet and Pamir Hindukush ranges, reproduced from Kumar et al. (2022), is shown for different depth sections—**a** 10 km, **b** 30 km, **c** 50 km and **d** 70 km. The reference velocity at each depth is indicated. The seismicity is represented by dots. The polygons represent different physical (red) and inferred (blue-dashed) features

Himalaya. Similarly, lateral variation of the coda wave attenuation in J & K Himalaya (Mitra et al. 2022) revealed higher attenuation at lateral heterogeneities, such as the Kishtwar window, Main Central thrust, etc., for low frequencies.

Eastern Himalaya and Indo-Burma ranges

Eastern Himalaya hosts the most diverse tectonics compared to other parts of the Himalaya which includes pop-up mechanism (Shillong Plateau), intraplate earthquakes (Kopili region), transverse motion (Sikkim), syntaxial bend, clockwise rotation of Brahmaputra valley (Vernant et al. 2014), etc. Therefore, understanding the internal structure of this region is important. RF H-κ stack performed for different stations distributed across northeast India (Kundu et al. 2020, 2022; Shukla et al. 2022) showed that H and σ vary from ~36 km to ~55 km and 0.23 to ~0.31, respectively. The thinnest crust and lowest σ are seen in the Brahmaputra Valley and Bengal Basin, while the thickest crust and largest σ are seen in the eastern margin of Arunachal Pradesh (close to the syntaxial bend) and Indo-Burma ranges. Joint inversion of RF with SW dispersion and RF CCP stacks at stations in the Arunachal Himalaya (Singh et al. 2021; Ravi Kumar et al. 2022) reveal a comparatively simpler crust with Moho depth and MHT linearly varying from 40 to 55 km and 10 to 20 km, respectively, at most places

(Fig. 3). A similar study for stations in the eastern margin of Arunachal Pradesh near the syntaxial bend (Kundu et al. 2023) observed identical Moho depth variation but slightly deeper MHT (~22–26 km).

By local earthquake tomography of the Shillong Plateau, Singh et al. (2022) reported that heterogeneities characterized by high V and low σ contributed towards the Shillong Plateau pop-up. Using a similar methodology, Mishra et al. (2023) delineated a gently north-dipping LVZ (MHT) at ~20 km depth in the Sikkim-Darjeeling Himalaya, which varies laterally. Local earthquake tomography (Mishra 2022) of northeast India and the Indo-Burma range and surface wave tomography of an even larger region, including southeastern Tibet (Kumar et al. 2021), revealed low-velocity sediments in the Bengal Basin, with its thickness increasing from the west to the east and high-velocity Indian slab steepening and underthrusting beneath the Burma arc. Kumar et al. (2021) also inferred oceanic crust beneath the Bengal Basin and continental crust beneath the Brahmaputra valley, Moho depth varying from ~40 km to ~70 km northwards from India to Tibet and indicated the role of collision geometry in lateral crustal thickness variation in Tibet. The spatial variation of coda wave attenuation in northeast India (Das and Mukhopadhyay 2020) showed that attenuation is highest in the Indo-Burma range, followed by those in the Mikir Hills and Shillong Plateau. This study also noted that

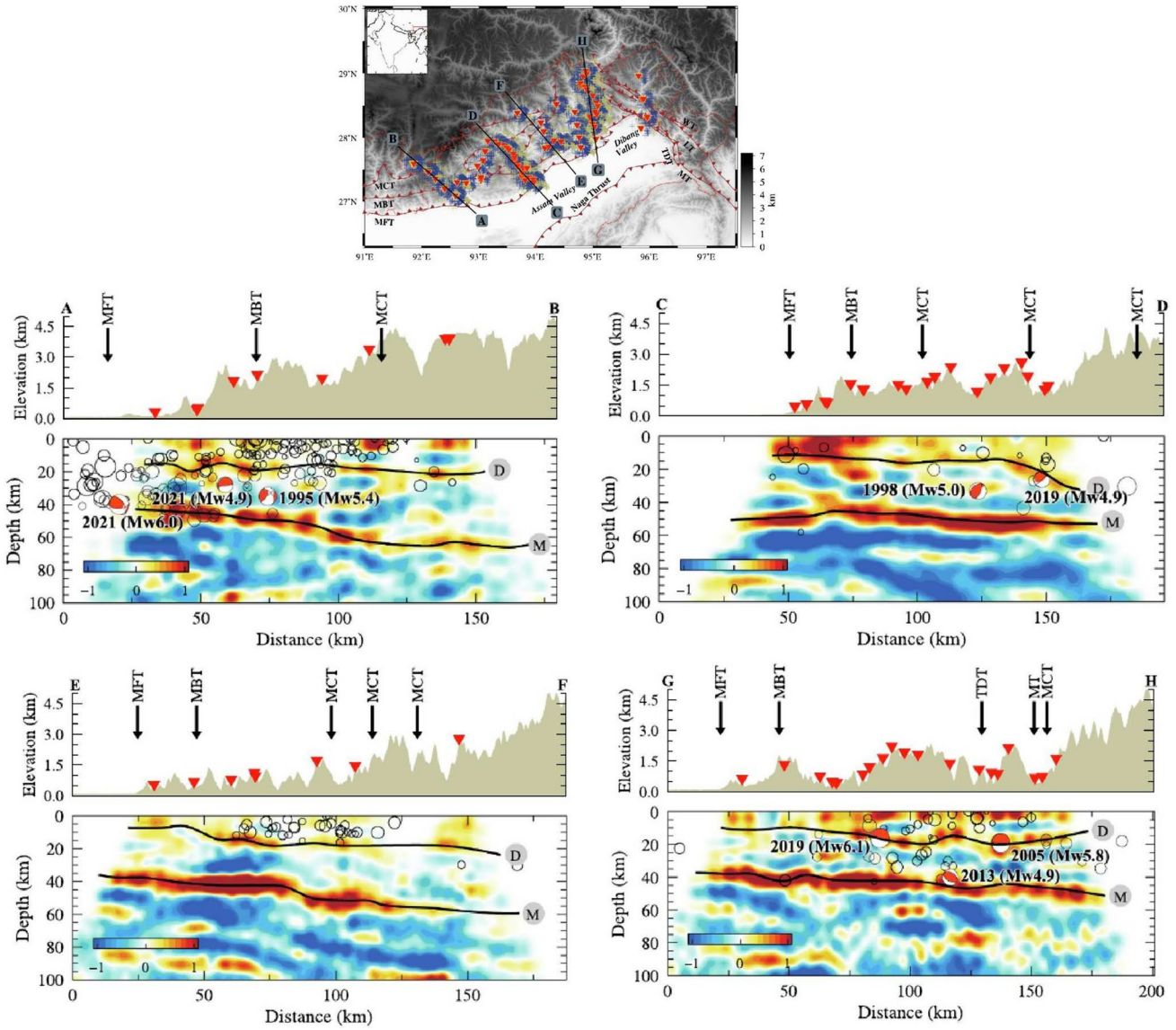

Fig. 3 RF migrated by 3D velocity model along four profiles AB, CD, EF and GH (inset) along with topography and station (red triangle) are reproduced from Ravi Kumar et al. (2022). The inferred MHT (D), Moho (M) and focal mechanisms of significant earthquakes are indicated. The earthquakes are shown as open circles

the attenuation gradient with depth varies from region to region.

The above studies mapped down to crust and upper mantle depths. However, there are a number of studies which imaged the deeper structures in this region. By RF CCP stacks and joint inversion of RF and SW dispersions, Chaudhury and Mitra (2023) mapped the Hales discontinuity (H-D) at depths 86–106 km beneath the Brahmaputra valley and Shillong Plateau. They inferred H-D to be a petrological boundary between mantle peridotite and kyanite-eclogite. Saikia et al. (2020) and Kumar et al. (2023a) imaged the topography of the Mantle Transition Zones (MTZ) using RF modelling beneath the Nepal & eastern Himalaya and adjoining regions (Fig. 4). They found that 410 km and 660 km discontinuities are uplifted by ~10–20 km almost everywhere across the Himalayan collision zone (including Nepal, Sikkim, Bhutan and Arunachal) possibly due to the presence of the thickened lithosphere. The 410 and 660 discontinuities are depressed beneath the Bengal Basin, northern and eastern Tibet, while an uplifted 410 discontinuity and depressed 660 discontinuity, observed beneath the Burmese arc, probably indicate the presence of lithospheric slabs within the MTZ. Travel-time tomography of the Arunachal Himalaya, Burmese arc and adjoining regions (Dubey et al. 2022) down to 1000 km revealed the extension of the Indian lithosphere upto Bangong–Nujiang Suture zone where it steeply descends down to 200 km along with a detached slab traced down to 600 km depth.

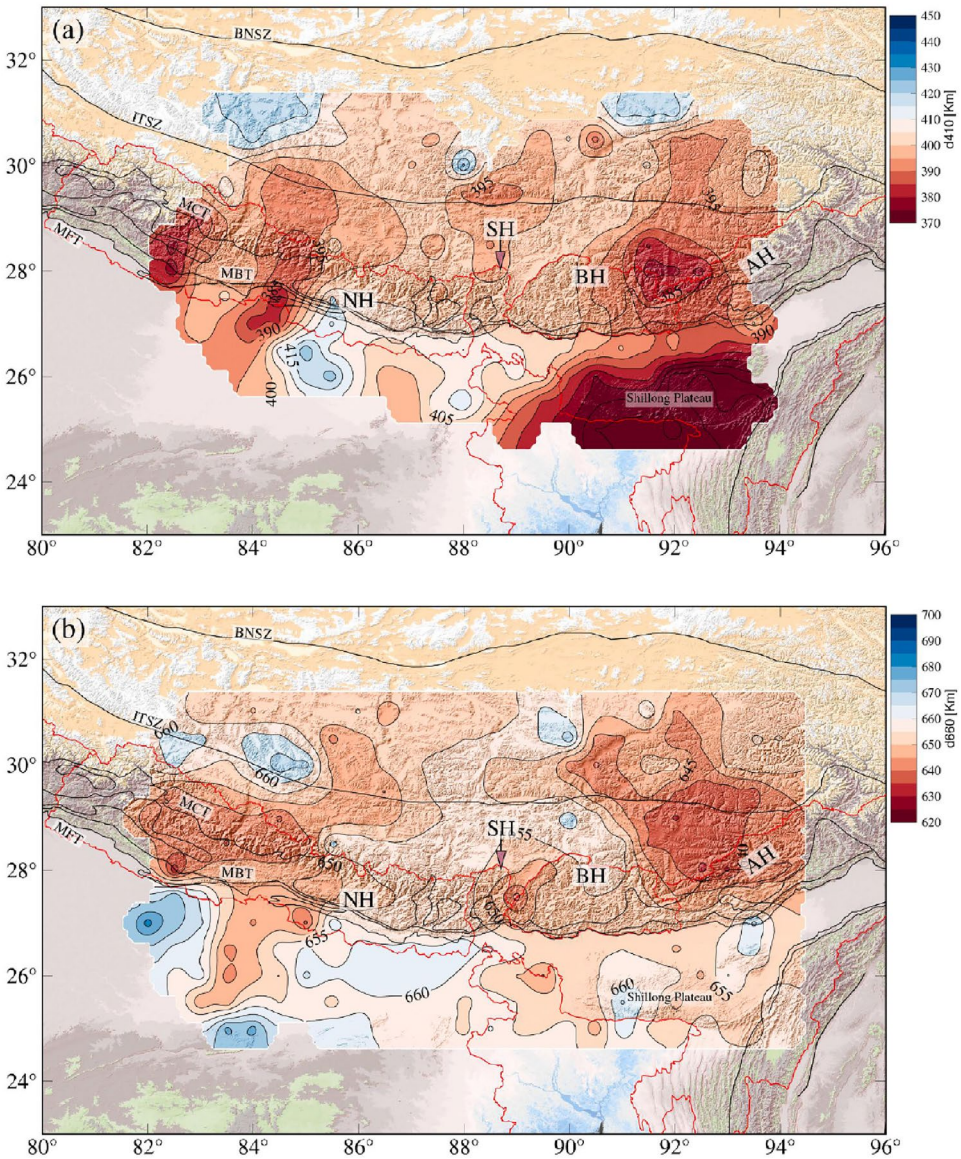

Fig. 4 Lateral variation of the depth of the **a** 410 km and **b** 660 km discontinuity reproduced from Kumar et al. (2023a, b). The MTZ topography variation in the Nepal Himalaya, Sikkim, Tibet and Bhutan is shown

Kachchh rift zone (KRZ) and adjoining regions

Kachchh Rift zone represents one of the reactivated Mesozoic rifts in the western margin of India. One of the largest intraplate earthquakes (M_W 7.7) occurred in this region in 2001, and since then minor to moderate seismicity has been continuing. Earlier studies of the region have shown marked thinning of the crust and lithosphere beneath the KRZ. Local earthquake tomography of KRZ (Mandal 2020, 2022a) revealed high velocity anomalies (both V_P and V_S) beneath the Banni and Wagad uplift regions at 10-40 km depths, possibly related to mafic plutons. These studies also showed low-velocity anomalies in the upper crust, mostly related to sedimentary structures. Earlier studies have shown that regions associated with larger earthquakes are characterized by low V_P, V_S and high V_P/V_S ratio. Although converted phase studies (RF) are usually (over)-utilised to estimate the Moho, an equally stronger phase – the reflected phase has never been exploited in the Indian scenario. For the first time, Paul et al. (2021) used Moho-reflected phases to image the crustal thickness and uppermost mantle velocities. This study showed that the uppermost mantle velocities beneath the KRZ are higher compared to that of Saurashtra, probably indicating a higher uppermost mantle temperature beneath the KRZ. This study also observed that the thin crust beneath the KRZ is underlain by a root (Fig. 5a, b). This root seems to be developed as a result of a change in

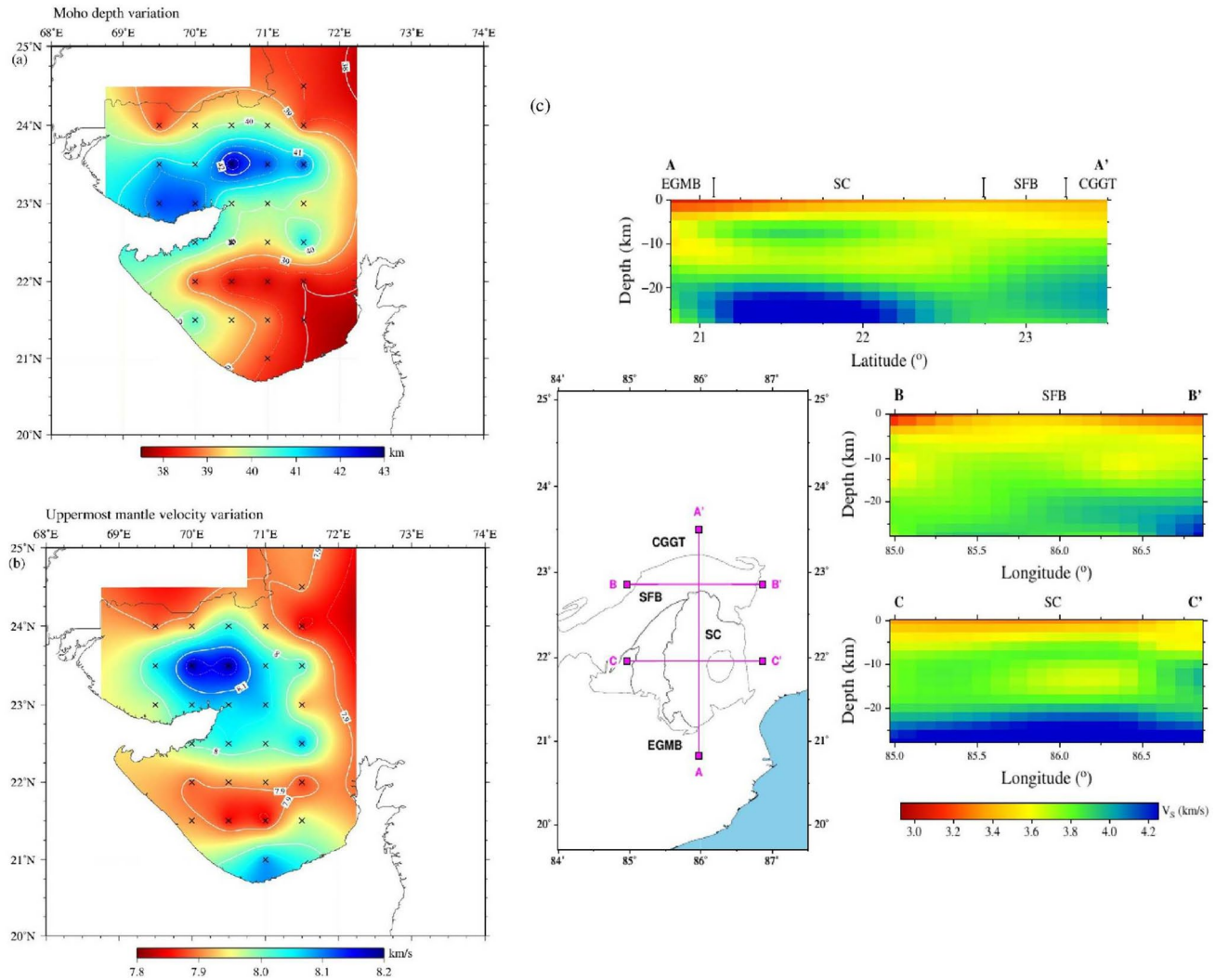

Fig. 5 **a** The Moho depth and **b** uppermost mantle velocity variation obtained from modelling of Moho-reflected P waves beneath the Gujarat region (reproduced from Paul et al. 2021) and **c** V_S variation in cross-sections along different profiles in the Eastern Shield (reproduced from Paul et al. 2024a) are shown. The data points are indicated by crosses in (**a**) and (**b**). Note that colour scales are different in (**a**–**c**)

regime from extensional to compressional between 65 and 50 Ma.

Indian Shield region

Eastern Indian Shield region

The Eastern Indian Shield comprising the Singhbhum craton (SC) and Chhotanagpur Granitic Gneissic Terrain (CGGT) is important in the sense that SC is the oldest craton within India which provides scope for understanding the evolution of the Archean crust. Additionally, there is a debate on the northward subduction of SC beneath the CGGT. Joint inversion of RF and SW dispersion (Mandal et al. 2021b) at 15 stations distributed across the SC, CGGT and northern part of the Eastern Ghat Mobile Belt (EGMB) indicated upwarping of the crust and lithosphere beneath the SC while they are relatively thicker beneath the CGGT. By RF H-κ and RF CCP images, Mandal (2022b) inferred the secular variation of the Archean crust formation and the northward subduction of the SC beneath the CGGT during the Precambrian. ANT using data from the same stations, Paul et al. (2024a) showed the presence of an ultramafic body in the lower crust beneath the SC while it was absent beneath adjoining regions (Fig. 5c). It is proposed that the ultramafic body is caused by ultra-high-temperature metamorphism in a lithosphere delamination setting.

South Indian Shield region

South Indian Shield consists of important geological provinces such as the Eastern and Western Dharwar Craton (EDC, WDC), Deccan Volcanic Province (DVP), Southern Granulite Terrain (SGT), Cudappah Basin (CB), Western Ghats (WG), EGMB, etc. Using RF H-κ stack and RF modelling, Kumar et al. (2020) showed the crust beneath the EDC is thinner (32–34 km) and has a sharp Moho compared to DVP which has a thicker (34–40 km) crust and gradational Moho. Studies involving SW tomography, along with joint inversion of RF with SW dispersion (Gupta and Kumar 2022; Chaubey et al. 2023) inferred a thick lithosphere (165–175 km) beneath the EDC, whereas it is seen to be thin (≤125 km) beneath the DVP and CB. The studies inferred that the DVP lithosphere is possibly altered, whereas that of EDC is undisturbed by Deccan volcanism. However, Mukherjee et al. (2022), based on seismological, thermal and available geochemical data, inferred that the lithosphere beneath the EDC is much thinner (78–125 km). It implies that an agreement on the lithosphere thickness beneath the Dharwar Craton is still lacking.

A high-resolution 3D V_S model obtained by SW tomography (Mullick et al. 2022) revealed a well-preserved Archean lithosphere (150–200 km thickness) beneath the northern Dharwar Craton (DC) with high V_S (4.7 km/s) at 50–100 km depths (Fig. 6). However, the lithosphere beneath the southern WDC and SGT were inferred to have undergone compositional changes and erosion, respectively. Teleseismic travel-time residual inversion (Kumar and Gupta 2023) showed the presence of high upper mantle velocities beneath the DC, possibly representing preserved or altered cratonic roots. A joint analysis of travel-time residuals with gravity and topography data (Arjun et al. 2022) revealed that the lithosphere of WDC is at least 20 km thicker than that of EDC and that the topographic load of the WG is supported by the DC. They also found lower effective elastic thickness of the EDC and WDC compared to neo-terrains like the IGP or Himalaya.

SW tomography and joint inversion of RF with SW dispersions across 27 stations (Jana et al. 2022) showed a thick crust (~45 km) and lithosphere (120–160 km) beneath the EGMB compared to those of the adjacent cratons (34–38 km and 90–120 km). The EGMB crust is also characterized by heterogeneous crust and gradational Moho, possibly owing to magmatic underplating. RF modelling and RF CCP images at 30 stations in the WG (Padma Rao and Ravi Kumar 2022a) showed that the crust is thick (45 km) beneath the central part while it thins in both north and south direction by ~6–8 km. The study also revealed a sub-Moho LVL and anisotropic/dipping nature of the Moho along the WG, possibly owing to past rifting episodes. Using RF CCP stack and joint inversion of RF with SW dispersion, Chaudhury et al. (2021) identified the H-D at 107–113 km beneath the EDC and ~102 km beneath the SGT. This study proposed the H-D to be subducted eclogitic oceanic crusts within the mantle peridotite.

Indian Ocean region

Joint inversion of RF with SW dispersion, complemented by gravity and magnetic data, showed that the crustal thickness of Amsterdam-St. Paul (ASP) plateau in the southern Indian Ocean varies from ~6–18 km and is comprised of 3 layers (Kumar et al. 2023b). This study finds the LAB of ASP at 50 km and a sub-Moho LVL at 20–36 km, possibly indicating magma material. A coda-wave attenuation study of the Indian Ocean region (Ekka et al. 2020) found significant variation in the attenuation parameters at different seismotectonic zones with the highest attenuation close to the Rodriguez Triple Junction.

Significant efforts have been made to image the deeper structure beneath the Indian Ocean, mainly to understand the enigmatic Indian Ocean Geoid Low (IOGL). Images obtained by the RF CCP stack revealed elevation of the 660 km discontinuity and a thin MTZ beneath the IOGL region, possibly suggesting anomalously high temperatures

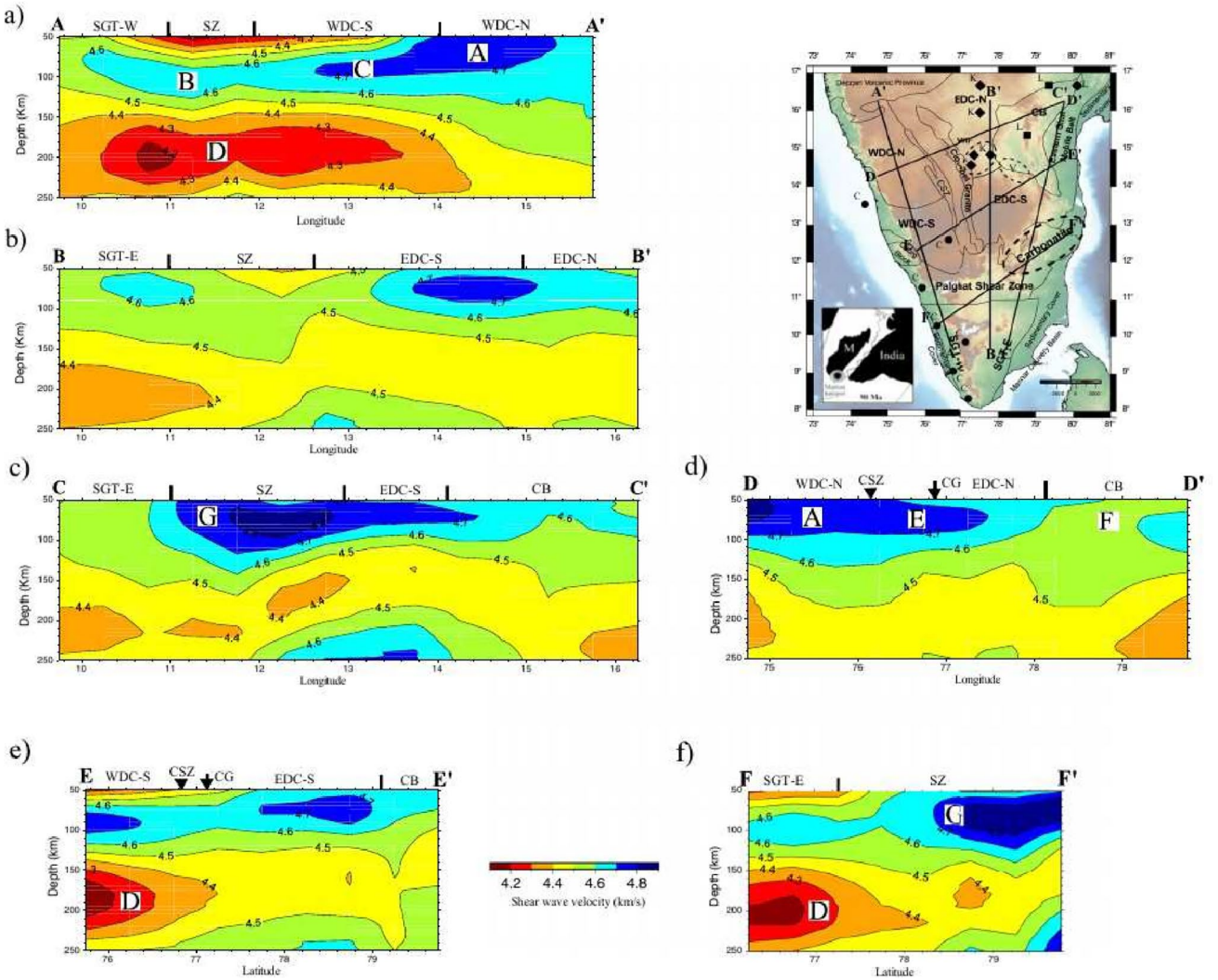

Fig. 6 V_S variation in cross-sections along different profiles in the South Indian Shield (inset) reproduced from Mullick et al. (2022)

of the mid mantle (Padma Rao et al. 2020). Modelling the differential of Core-reflected P- and S-phases with the direct P- and S-phases, Padma Rao and Ravi Kumar (2022b) found positive perturbations beneath the IOGL region (Fig. 7). They inferred high velocity of the D'' layer atop the Core-Mantle Boundary (CMB), possibly representing subducted slabs. By cluster analysis and vote-map analysis of global tomographic models, Paul and Ravi Kumar (2022) showed that low-velocity anomalies exist in the upper mantle beneath the IOGL and Ross Sea regions, whereas high-velocity materials, inconsistent in dimension and orientation, lie in the lower mantle. They also identified a consistently low velocity structure throughout the mantle, probably representing a plume arising from the edge of the African Large Low Shear-wave Velocity province to the upper mantle beneath the IOGL.

Other regions

A high-resolution 3D V_S model obtained by SW tomography beneath the Bay of Bengal region (Saha et al. 2021) revealed a distinct lithosphere that is thicker (>120 km) in the western part and thinner in the eastern part (60–75 km). They interpreted the thickening to be due to the conductive cooling of an oceanic plate. High-frequency ANT of 20 stations around the Lonar crater in the DVP revealed that the impact crater is an LVZ with a depth extent of ~500 m and is consistent with the scaling of global simple craters (Kumar and Rai 2023). By grid-searching for V_P and V_P/V_S ratio and synthesizing hundreds of models to minimize the travel-time residuals, Paul et al. (2024b) showed that the Palghar seismic zone, a site for recent induced seismicity on the western coast of India, has a low V_P and high $V_P/$

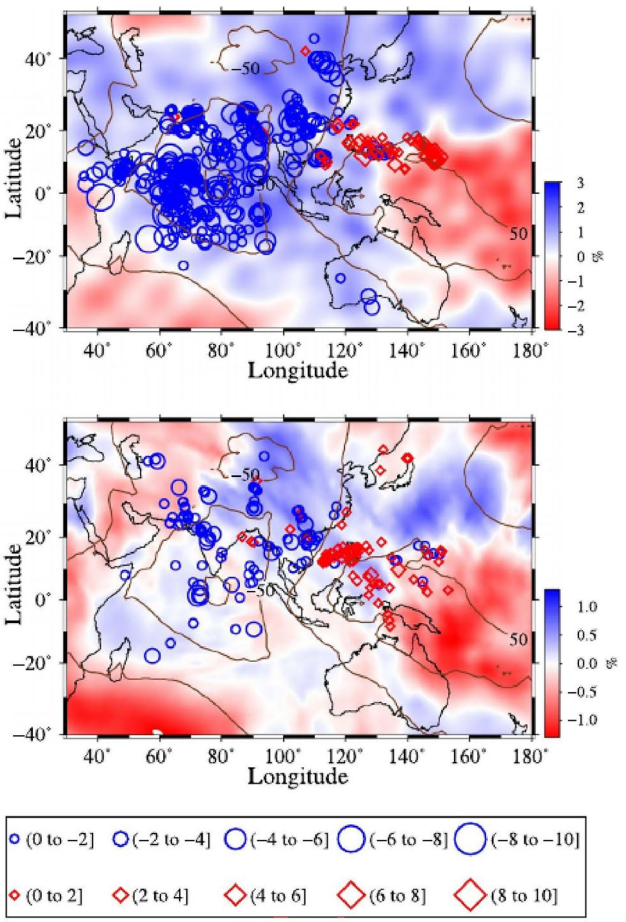

Fig. 7 Reproduced from Padma Rao and Ravi Kumar (2022b). The observed travel-time differential of direct S and core-reflected S (top panel) and direct P and core-reflected P phases (bottom panel) wrt to corresponding differentials predicted from the PREM model are shown by circle (negative) and diamond (positive) shapes. The size of the shapes is scaled by the magnitude of travel-time residuals. The backgrounds are velocity perturbations from global velocity models—S40RTS (top) and LLNL-G3Dv3 (bottom)

V_S ratio, possibly indicating the role of fluids (rainfall) in generating the earthquakes. A seismic attenuation study in the Andaman Nicobar subduction zone (Dutta et al. 2021) showed a highly attenuative crust and upper mantle and that the attenuation is higher in the northern part compared to the southern part. Dutta et al. (2021) also reported that energy decay is dominated by intrinsic attenuation, and it remains almost constant at 115–132 km depths.

Pan-India studies

Generally, local or regional studies provide higher resolution images that distinguish minute depth variations of discontinuities or velocity properties of the crust and mantle. However, imaging at global or continent/sub-continent level is important to understand the broad-scale variation between different units. 3D V_S model obtained by AN and SW tomography (Saha et al. 2020) revealed that peninsular India can be divided into a homogeneous (in WDC, eastern DVP and Marwar block) and a two-layered lithosphere (in EDC, SC, CGGT, Bastar Craton, Bundelkhand craton and Vindhya Basin). This study observed that the lithosphere thickness varies between 100 and 180 km in peninsular India, with the thinnest part in western DVP, and it inferred the segmentation of the lithospheric block beneath the IGP by several N–S trending ridges. RF modelling at 23 stations across the Indian Shield showed that the thickness of MTZ beneath most of the Indian cratons matches well with that of the global average (Kharita and Mukhopadhyay 2023). This study found a persistent and laterally varying mid-transition zone discontinuity and distinguished regions with a probable larger weight percentage of water in the MTZ.

Pn tomography of the Indian Shield (Illa et al. 2021a) shows a large variation of the uppermost mantle velocity with a mean of 8.22 km/s, slightly higher than the global average. The collision zones in the Himalaya, Tibet, Tarim Basin and Indo-Burma arc are characterized by high Pn values. The Pn is also high beneath the central Indian Shield, possibly due to the presence of mafic magma related to Deccan volcanism. Similarly, Sn tomography (Illa et al. 2021b) showed an average Sn of 4.6 km/s with higher Sn in central India, DVP, SGT, CB, Himalaya and Tarim Basin, possibly indicating a cold lithosphere. Contrasting Sn is seen beneath the western and eastern parts of the DC and Bay of Bengal. Lg wave attenuation tomography across the Indian Shield (Reshma et al. 2022) showed a large variation of the Quality factor, with the highest attenuation seen in rifts, sutures, sedimentary and active zones, while the cratons showed lower attenuation except in southern DC to SGT. By RF CCP images, Srinu et al. (2021) revealed the X-discontinuity (a seismic discontinuity) as a sporadic and thin feature in the 246–355 km depth range beneath India and it is uncorrelated with either MTZ or tectonic regions (Fig. 8). This study suggested its origin owing to Orthoenstatite to Clinoenstatite transformation and coestite-stishovite transition at high pressure.

Summary

From the above discussions, it is seen that a large number of seismological imaging studies has been performed in the last 4 years which comprehensively exceeds the number of publications on the subject in the previous 4-year period (2015–2019). The studies showed high-resolution imaging in different regions, although the seismological imaging studies carried out in the Himalaya exceed such studies in any other part of India. Exceptional progress has been made in imaging the MHT, especially confirmation

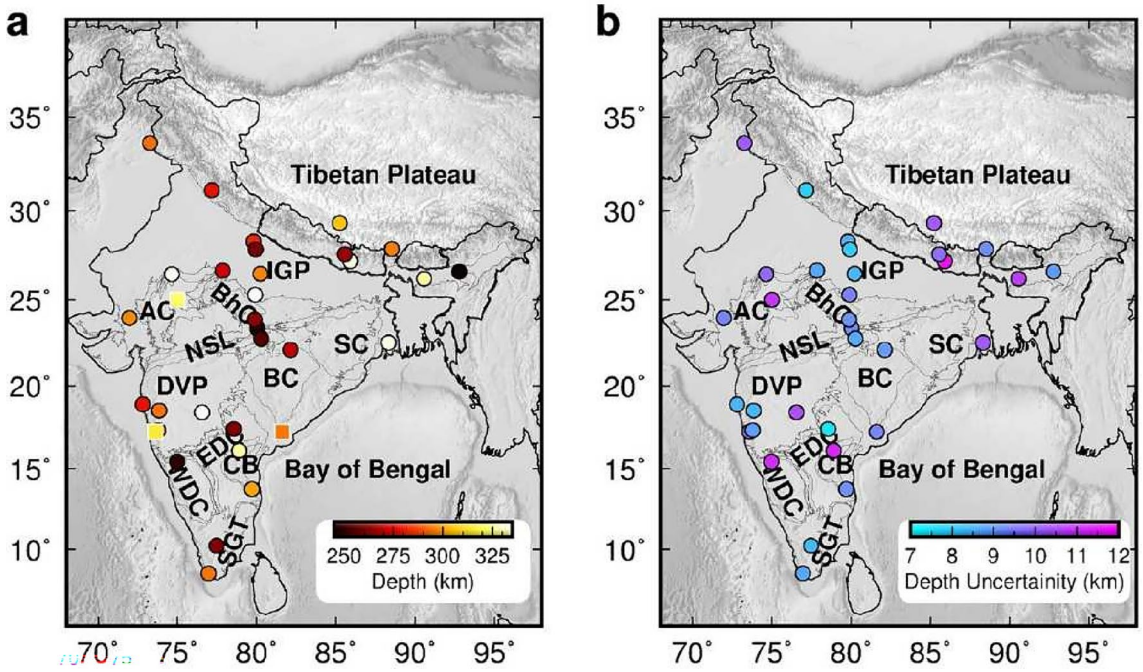

Fig. 8 The **a** depth and **b** uncertainty of X-discontinuity beneath India is shown (reproduced from Srinu et al. 2021). A square shape is shown where a probable double X-phase is observed

of its flat-ramp-flat geometry in almost all parts of the Himalaya, with the exception of Arunachal Himalaya, where the MHT is flat. Duplex structures are seen to be existent in some parts like the J & K and Himachal Himalaya. Moho depth estimation has been carried out in almost all regions of India, with dense coverage of stations and it seems a general notion about its depth range, geometry and velocity characteristics has been well-established. Many studies mapped the LAB depth both by RF modelling and tomography, specifically in the Uttarakhand region, Kachchh, Singhbhum and South Indian Shield. However, contrasting results have been obtained regarding the lithosphere thickness of the DC. It is also encouraging to see a significant number of studies attempting to image the deeper structures such as H-D, MTZ, X-discontinuity and D'' layer atop the CMB. Studies have been able to identify anomalies present in the crust, sub-Moho or within the lithosphere with greater accuracy. Seismic attenuation structure, which is important for hazard analysis, has been mapped in most parts of the Himalaya, Indian Ocean region, Andaman region and also at the pan-India level. Although a high-resolution seismic image of the Indian subcontinent is gradually becoming available, it is seen that most studies are limited to seismic imaging and possible interpretations of the obtained structure. Efforts have not been made towards a geodynamical or theoretical understanding of the associated processes or forces shaping the structure.

Appendix A

A Brief Note on the different seismic imaging techniques frequently used in the text.

Receiver functions (RF)

A Receiver function is obtained by deconvolving the radial component waveform from the vertical component of a teleseismic (epicentral distance 30°–90°) earthquake. It contains information about phases such as the P-to-s converted phase and multiply reflected phases, which are characteristics of the discontinuity beneath the receiver.

RF modelling/inversion

RF modelling usually involves a linearized inversion scheme to obtain a 1D V_S model which could fit the observed RF waveform with a minimum misfit. The depth and velocity contrast across the discontinuity are reliable in an RF inversion, while the absolute velocity is less constrained.

RF H-κ stack

The delay time of the P-to-s converted and reflected phases is a function of the depth of the discontinuity (H) and V_P/

V_S ratio (κ) of the crust. By grid-searching H and κ, the values are chosen at which the sum of the amplitudes of the converted and reflected phase is maximum.

Poisson's ratio (σ) gives the ratio of transverse strain to longitudinal strain and is related to κ as $\sigma = (\kappa^2 - 2)/(2\kappa^2 - 2)$.

Surface wave dispersion

Surface waves (SW) of different frequencies travel with different velocities. The relation between frequency (or time period) and velocity is called dispersion and is usually seen as a listric curve.

If group velocity of the surface wave is measured, it is called group velocity dispersion. Similarly, phase velocity dispersion is named. Similarly, if Rayleigh/Love surface waves are used, they are called Rayleigh/Love wave dispersion, and it can be more specific as Rayleigh wave group velocity dispersion, etc.

Surface wave inversion

A linearized inversion scheme to obtain a 1D shear-wave velocity model by matching the observed dispersion with a minimum misfit.

Joint inversion of RF and SW dispersion

RF is sensitive to the impedance contrast, whereas SW is sensitive to average velocity variation along the propagation path. In order to make use of both sensitivities, a joint inversion by assigning different weights to both datasets is carried out, generally, by a linearized scheme to obtain a 1D V_S model, which provides a good estimation of the depth of the discontinuities as well as their velocities.

RF common conversion point (CCP) stack

RF CCP stack involves depth migration of the RF by a 1D or 3D model. In this technique, individual RFs are projected along a given cross-section through their piercing point, and the travel-times of different phases are converted to depth according to the velocity model. RF amplitudes are stacked in small resolution bins if required.

Tomographic inversion

In tomographic inversion, a given uniform velocity model is perturbed iteratively to match the observed and predicted travel times along different paths. Based on the phase or process from which the travel-time is obtained, the tomography nomenclature is done accordingly. For example, if P-phase travel-times are obtained from local earthquakes, then the tomography can be named local earthquake body wave tomography. Similarly, there can be teleseismic earthquake tomography, Rayleigh/Love wave group-velocity/phase velocity tomography, Pn/Sn-tomography, etc. The inversion scheme may vary for different tomography studies.

Ambient noise tomography (ANT)

ANT is similar to SW tomography, where group/phase velocity travel-times are inverted to obtain a tomography map with an additional preceding step. Cross-correlation of ambient noise is performed to obtain an Empirical Green's function, which is similar to a surface wave.

1D V_S model can be obtained by inverting dispersion curves extracted from regular grids of SW or AN tomography maps. The 1D models can be joined together to form a 3D V_S model.

Seismic attenuation

Seismic attenuation is defined as the ratio of lost energy to total energy per energy cycle. The amplitude of a seismic wave attenuates exponentially and can be obtained by modelling the spectra, as the attenuation factor is proportional to the slope of the power spectra. Attenuation of different phases viz. P-, S- and coda waves differ.

Appendix B

Full forms of the frequently used abbreviations.

ANT	Ambient noise tomography
AN	Ambient noise
CB	Cuddapah basin
CCP	Common conversion point
CGGT	Chhotanagpur granitic gneissic terrain
CMB	Core-mantle boundary
DC	Dharwar craton
DVP	Deccan volcanic province
EDC	Eastern Dharwar Craton
EGMB	Eastern ghat mobile belt
H–D	Hales discontinuity
IGP	Indo-gangetic plains
IOGL	Indian ocean geoid low
KRZ	Kachchh rift zone
LVL	Low-velocity layer
LVZ	Low-velocity zone
MHT	Main Himalayan thrust
MTZ	Mantle transition zone
RF	Receiver function
SC	Singhbhum craton
SGT	Southern granulite terrain
SW	Surface wave

WDC Western Dharwar Craton
WG Western ghats

Declarations

Conflict of interest The authors declare that there is no conflict of interest.

References

Arjun, V.H., Gupta, S., Tiwari, V.M.: Lithospheric structure of the Dharwar Craton (India) from joint analysis of gravity, topography, and teleseismic travel-time residuals. J. Asian Earth Sci. **239**, 105397 (2022)

Ashish, S.G., Rai, S.S.: 3-D crustal structure in Kumaon-Garhwal Himalaya using joint inversion of receiver functions and surface wave group velocity. Geophys. J. Int. **233**, 2101–2123 (2023)

Bilham, R., Wallace, K.: Future MW>8 earthquakes in the Himalaya: Implications from the 26 Dec 2004 MW=9.0 earthquake on India's eastern Plate margin. Geol. Surv. India Spec. Publ.Surv. India Spec. Publ. **85**, 1–14 (2005)

Chaubey, D.K., Rai, S.S., Mullick, N., Das, R.: Lithospheric structure beneath the eastern Dharwar craton kimberlite field, India, inferred from joint inversion of surface wave dispersion and receiver function data. Precambrian Res. **394**, 107112 (2023)

Chaudhury, J., Mitra, S.: Subcontinental lithospheric mantle discontinuities beneath the Eastern Himalaya plate boundary system, NE India. Geophys. J. Int. **233**, 2155–2171 (2023)

Chaudhury, J., Mitra, S., Sarkar, T.: Hales discontinuity in the southern Indian continental lithosphere: Seismological and petrological models. J. Geophys. Res.Geophys. Res. **126**, e2020JB02056 (2021)

Das, R., Mukhopadhyay, S.: Regional variation of coda wave attenuation in Northeast India: an understanding of the physical state of the medium. Phys. Earth Planet. Inter. **299**, 106404 (2020)

Dubey, A.K., Singh, A., Ravi Kumar, M., Jana, N., Sarkar, S., Saikia, D., Singh, C.: Tomographic imaging of the plate geometry beneath the Arunachal Himalaya and Burmese subduction zones. Geophys. Res. Lett.. Res. Lett. **49**, e2022GL098331 (2022)

Dutta, A., Biswas, R., Singh, C., Ravi Kumar, M., Jana, N., Singh, A.: Depth-wise attenuation mechanism of seismic waves in the Andaman region. Soil Dyn. Earthq. Eng. **151**, 107000 (2021)

Ekka, M.S., Vandana, R.P.N.S., Mishra, O.P.: Coda wave seismic structure beneath the Indian Ocean region and its implications to seismotectonics and structural heterogeneity. J. Asian Earth Sci. **188**, 104104 (2020)

Gupta, S., Kumar, S.: Lithosphere thickness variation across the Deccan Volcanic Province – Eastern Dharwar Craton, South India: Insight into evolution of the Deccan Volcanic Province. J. Earth Syst. Sci. **131**, 10 (2022)

Gupta, S., Mahesh, P., Kanna, N., Sivaram, K., Paul, A.: 3-D seismic velocity structure of the Kumaun-Garhwal (Central) Himalaya: insight into the Main Himalayan Thrust and earthquake occurrence. Geophys. J. Int. **229**, 138–149 (2022)

Hazarika, D., Hajra, S., Kundu, A., Bankhwal, M., Kumar, N., Pant, C.C.: Imaging the Moho and Main Himalayan Thrust beneath the Kumaon Himalaya: constraints from receiver function analysis. Geophys. J. Int. **224**, 858–870 (2021)

Illa, B., Reshma, K.S., Kumar, P., Srinagesh, D., Halder, C., Kumar, S., Mandal, P.: Pn tomography and anisotropic study of the Indian shield and the adjacent regions. Tectonophys. **813**, 228932 (2021a)

Illa, B., Kumar, P., Reshma, K.S., Srinu, U., Srinagesh, D.: Sn wave tomography of the uppermost mantle beneath the Indian Shield and its adjacent regions. Phys. Earth Planet. Inter. **319**, 106785 (2021b)

Jana, N., Singh, C., Singh, A., Eken, T., Dubey, A.K., Dutta, A., Gupta, A.K.: Lithospheric architecture below the Eastern Ghats Mobile Belt and adjoining Archean Cratons: imprints of India-Antarctica collision tectonics. Gondwana Res. **111**, 209–222 (2022)

Kanaujia, J., Ravi Kumar, M., Vijayaraghavan, R., Solomon Raju, P.: An optimum 1D velocity model for the Garhwal-Kumaun Himalaya using Monte Carlo style inversion. Seismol. Res. Lett. **94**(5), 2244–2256 (2023)

Kanna, N., Gupta, S.: Crustal seismic structure beneath the Garhwal Himalaya using regional and teleseismic waveform modelling. Geophys. J. Int. **222**, 2040–2052 (2020)

Kanna, N., Gupta, S.: Seismic crustal shear velocity structure across NW Himalaya and Ladakh-Karakoram using receiver function modelling: Evidence of the Main Himalayan Thrust. Phys. Earth Planet. Inter. **311**, 106642 (2021)

Kharita, A., Mukhopadhyay, S.: Wet mantle transition zone beneath the Indian shield: constraints from P-to-S receiver function analysis. Phys. Earth Planet. Inter. **341**, 107049 (2023)

Kumar, S., Gupta, S.: Insights into the evolution of the Dharwar craton, South India through three dimensional P-wave velocity imaging of upper mantle. J. Asian Earth Sci. **251**, 105655 (2023)

Kumar, V., Rai, S.S.: 3-D geometry of the Lonar impact crater, India, imaged from cultural seismic noise. Geophys. J. Int. **234**, 1933–1942 (2023)

Kumar, S., Gupta, S., Kanna, N., Sivaram, K.: Crustal structure across the Deccan Volcanic province and Eastern Dharwar Craton in south Indian shield using receiver function modelling. Phys. Earth Planet. Inter. **306**, 106543 (2020)

Kumar, A., Kumar, N., Mukhopadhyay, S., Klemperer, S.L.: Image of shear wave structure of NE India based on analysis of Rayleigh wave data. Front. Earth Sci. **9**, 680361 (2021)

Kumar, V., Rai, S.S., Hawkins, R., Bodin, T.: Seismic imaging of crust beneath the western Tibet-Pamir and western Himalaya using ambient noise and earthquake data. J. Geophys. Res.Geophys. Res. **127**, e2021JB022574 (2022)

Kumar, G., Singh, A., Tiwari, A.K., Singh, C., Ravi Kumar, M., Saikia, D., Uthaman, M., Dubey, A.K.: Alteration in the mantle transition zone structure beneath Sikkim and adjoining Himalaya in response to the Indian plate subduction. J. Asian Earth Sci. **255**, 105768 (2023a)

Kumar, P., Singha, P., Ghosal, D., Jacob, J., Gupta, S.: Lithospheric architecture beneath the Amsterdam-St. Paul plateau, Southern Indian Ocean using the integrated gravity, magnetic and seismological study. Tectonophysics **863**, 229989 (2023b)

Kumari, R., Kumar, P., Kumar, N., Sandeep,: Role of site effect for the evaluation of attenuation characteristics of P, S and coda waves in Kinnaur region, NW Himalaya. J. Earth Syst. Sci. **129**, 191 (2020)

Kundu, A., Hazarika, D., Hajra, S., Singh, A.K., Ghosh, P.: Crustal thickness and Poisson's ratio variations in the northeast India-Asia collision zone: Insight into the Tuting-Tidding Suture zone, eastern Himalaya. J. Asian Earth Sci. **188**, 104099 (2020)

Kundu, A., Hazarika, D., Yadav, D.K., Ghosh, P.: Crustal thickness and Poisson's ratio variations in the Siang Window and adjoining areas of the Eastern Himalayan Syntaxis. J. Asian Earth Sci. **231**, 105225 (2022)

Kundu, A., Hazarika, D., Hajra, S., Yadav, D.K.: Imaging the crustal structure at the northeast corner of the indenting Indian Plate in the Eastern Himalayan Syntaxis. Geophys. J. Int. **235**, 1035–1048 (2023)

Madhusudhan, S., Gupta, S., Kanna, N., Kumar, S., Sivaram, K.: Seismic characteristics of the underthrusting Indian lithosphere beneath

the eastern Kumaon Himalaya using regional earthquake waveform analysis. J. Asian Earth Sci. **237**, 105356 (2022)
Mandal, P.: Three-dimensional seismic velocity imaging of the Kachchh rift zone, Gujarat, India: Implications toward the crustal mafic pluton induced intraplate seismicity. J. Asian Earth Sci. **192**, 104226 (2020)
Mandal, P.: Seismic velocity images of a crystallized crustal magma-conduit (related to the Deccan plume) below the seismically active Kachchh rift zone, Gujarat, India. Nat. Haz. **111**, 239–260 (2022a)
Mandal, P.: Evidence of secular variation in Archean crust formation in the Eastern Indian Shield. Sci. Rep. **12**, 14040 (2022b)
Mandal, P.: The Uttarakhand Himalaya: An image of the main Himalayan thrust, Moho, and lithosphere-asthenosphere boundary. J. Asian Earth Sci. **253**, 106724 (2023)
Mandal, P., Srinivas, D., Suresh, G., Srinagesh, D.: Modelling of crustal composition and Moho depths and their Implications toward seismogenesis in the Kumaon-Garhwal Himalaya. Sci. Rep. **11**, 14067 (2021a)
Mandal, P., Kumar, P., Sreenivas, B., Babu, E.V.S.S.K., Bhaskar Rao, Y.J.: Variations in crustal and lithospheric structure across the Eastern Indian Shield from passive seismic source imaging: Implications to changes in the tectonic regimes and crustal accretion through the Precambrian. Precambrian Res. **360**, 106207 (2021b)
Mandal, P., Srinagesh, D., Vijayaraghavan, R., Suresh, G., Naresh, B., Solomon Raju, P., Devi, A., Swathi, K., Singh, D.K., Srinivas, D., Saha, S., Shekar, M., Sarma, A.N.S., Murthy, Y.V.V.B.S.N.: Seismic velocity imaging of the Kumaon-Garhwal Himalaya, India. Nat. Haz. **111**, 2241–2260 (2022)
Mandal, P., Prathigadapa, R., Srinivas, D., Saha, S., Saha, G.: Evidence of structural segmentation of the Uttarakhand Himalaya and its implication for earthquake hazard. Sci. Rep. **13**, 2079 (2023)
Mishra, O.P.: Lithospheric heterogeneities of northeast India and Indo-Burma region: Geodynamic implications. Geosyst. Geoenviron. **1**, 100042 (2022)
Mishra, O.P., Vandana, K.V., Gera, S.K.: A new insight into seismic attenuation of Northwest Himalaya and its surrounding region: Implications to structural heterogeneities and earthquake hazards. Phys. Earth Planet. Inter. **306**, 106500 (2020)
Mishra, O.P., Singh, A.P., Singh, O.P.: Seismicity and decollement geometry beneath the Sikkim-Darjeeling Himalaya using local earthquake tomography: implications for seismotectonic and seismogenesis. Phys. Earth Planet. Inter. **336**, 106999 (2023)
Mitra, S., Wanchoo, S.K., Priestley, K.: Seismic coda-wave attenuation tomography of the Jammu and Kashmir Himalaya. J. Geophys. Res. Geophys. Res. **127**, e2022JB024917 (2022)
Mitra, S., Sharma, S., Wanchoo, S.K., Priestley, K.: 3D crustal structure of the Jammu and Kashmir Himalaya: signatures of mid-crustal ramp and Lesser Himalayan duplex. J. Geophys. Res.Geophys. Res **128**, e2023JB027350 (2023)
Monika, K.P., Sandeep, K.S., Joshi, A., Devi, S.: Spatial variability studies of attenuation characteristics of Q_α and Q_β in Kumaon and Garhwal region of NW Himalaya. Nat. Haz. **103**, 1219–1237 (2020)
Mullick, N., Rai, S.S., Saha, G.: Lithospheric structure of the South India Precambrian terrains from surface wave tomography. J. Geophys. Res.Geophys. Res **127**, e2022JB024244 (2022)
Mukherjee, S., Ray, L., Maurya, S., Shalivahan, P.K.: Nature of the lithosphere-asthenosphere boundary beneath the Eastern Dharwar Craton of the Indian Shield. J. Asian Earth Sci. **227**, 105071 (2022)
Padmarao, B., Ravi, K.M., Saikia, D.: Seismic evidence for a hot mantle transition zone beneath the Indian Ocean Geoid Low. Geochem. Geophys. Geosys. **21**, e2020GC009079 (2020)
Padma Rao, B., Ravi Kumar, M.: Evolution of the Western Ghats: constraints from receiver function imaging and harmonic decomposition. Tectonophys. **838**, 229472 (2022a)
Padma Rao, B., Ravi Kumar, M.: Lowermost mantle (D'' layer) structure beneath the Indian Ocean: insights from modeling of ScS-S and PcP-P residuals. J. Asian Earth Sci. **225**, 105038 (2022b)
Paul, H., Pandey, A., Ravi Kumar, M., Kumar, S.: Investigation of crustal thickness and uppermost mantle velocity beneath Gujarat, western India, utilizing Moho reflected P phases. Phys. Earth Planet. Inter. **310**, 106619 (2021)
Paul, H., Ravi Kumar, M.: Strong influence of tomographic models on geoid prediction: case studies from Indian Ocean and Ross Sea geoids. Tectonophysics **836**, 229429 (2022)
Paul, H., Singh, B., Mandal, P.: 3D shear-wave velocity structure of the Eastern Indian Shield from ambient noise tomography: Ultramafic lower crust underneath the Singhbhum Craton. J. Asian Earth Sci. **260**(1): 105954 (2024a). https://doi.org/10.1016/j.jseaes.2023.105954
Paul, H., Sunilkumar, T.C., Gahalaut, V.K., Srinagesh, D., Shekar, M.: Significance of VP/VS ratio in locating earthquakes of a long-duration swarm in the western coast of India. J. Seismol.Seismol. (2024b). https://doi.org/10.21203/rs.3.rs-2952593
Ravi Kumar, M., Padmarao, B., Mahesh, P., Venkatesh, V.: Scattered wave imaging of the Main Himalayan Thrust and mid-crustal ramp beneath the Arunachal and its relation to seismicity. J. Asian Earth Sci. **236**, 105335 (2022)
Reshma, K.S., Illa, B., Kumar, P., Srinagesh, D.: Lg Q in the Indian Shield, Pure Appl. Geophys. **179**, 149–168 (2022)
Saha, G.K., Prakasam, K.S., Rai, S.S.: Diversity in the peninsular Indian lithosphere revealed from ambient noise and earthquake tomography. Phys. Earth Planet. Inter. **306**, 106523 (2020)
Saha, G.K., Rai, S.S., Prakasam, K.S., Gaur, V.K.: Distinct lithosphere in the Bay of Bengal inferred from ambient noise and earthquake tomography. Tectonophysics **809**, 228855 (2021)
Saikia, D., Ravi Kumar, M., Singh, A.: Paleoslab and plume signatures in the mantle transition zone beneath Eastern Himalaya and adjoining regions. Geophys. J. Int. **221**, 468–477 (2020)
Shukla, N., Hazarika, D., Kundu, A., Mukhopadhyay, S.: Spatial variations of crustal thickness and Poisson's ratio in the northeastern region of India based on receiver function analysis. Geol. J. **57**, 5083–5096 (2022)
Singh, A., Saikia, D., Ravi Kumar, M.: Seismic imaging of the crust beneath Arunachal Himalaya. J. Geophys. Res.Geophys. Res **126**, e2020JB020616 (2021)
Singh, A.P., Mishra, O.P., Singh, O.P.: Seismic evidence of pop-up tectonics beneath the Shillong Plateau area of northeast India. Sci. Rep. **12**, 14135 (2022)
Sivaram, K., Gupta, S.: Frequency-dependent attenuation characteristics of coda and body wave in the Kumaon Himalaya: Implications for regional geology and seismic hazards. Pure Appl. Geophys.Geophys. **179**, 949–972 (2022)
Srinu, U., Kumar, P., Halder, C., Ravi Kumar, M., Srinagesh, D., Illa, B.: X-discontinuity beneath the Indian Shield—evidence for remnant Tethyan oceanic lithosphere in the mantle. J. Geophys. Res.Geophys. Res **126**, e2021JB021890 (2021)
Verma, S.K., Kumar, N., Hazarika, D., Paul, A., Yadav, D.K., Pal, S.K.: Shear wave crustal velocity structure in the Garhwal-Kumaon Himalaya based on noise cross-correlation of Rayleigh wave. Tectonophysis **866**, 230047 (2023)
Vernant, P., Bilham, R., Szeliga, W., Drupka, D., Kalita, S., Bhattacharya, A.K., Gaur, V.K., Pelgay, P., Cattin, R., Berthet, T.: Clockwise rotation of the Brahmaputra Valley relative to India: Tectonic convergence in the eastern Himalaya, Naga Hills and Shillong Plateau. J. Geophys. Res.Geophys. Res **119**(8), 6558–6571 (2014)